TÉLÉCOM SUDPARIS

OPTIMIZATION OF SHORT-RANGE OPTICAL LINKS FOR DATACENTER OR END-USER APPLICATIONS

Master Of Science Electrical and Optical Engineering

Javier Suárez Geijo

Tutor: Yann Frignac

March 2014

ABSTRACT

This project is a study of the optimization of a ring resonator filter situated after a DML semiconductor laser in a global short-range optical link system. The main purpose is to optimize the optical filter performing matlab simulations in order to find the parameters of the transfer function of the filter that we may tune to achieve an error-free transmission.

From a theoretical point of view, this project will give the knowledge of the optical direct modulation operation where the chirp is an evitable factor that we have to minimize to achieve good performance in our global system. Also a high extinction ratio over this low chirp will be an interesting parameter to take into account.

Combining the theoretical background of DML and ring resonators of terms such as FSR, internal losses, finesse…with the experimental work, the goal of the project will be achieved concluding that there is some intervals in which the parameters can oscillate in order to obtain the fewer errors in the system.

Table of Contents

1. INTRODUCTION

Future installation of short-range optical interconnects for datacenter or home application motivates manufacturers of direct modulated optical source to optimize their device design to reach more than 100 km error-free transmission. Considering the worldwide production of such sources to equip end-users or datacenters wherever the high bit rate transmission is needed, the hard constraint is to make it with the lowest price and energy consumption as possible. Among good candidates for such short-range optical links is the Intensity Modulation-Direct Detection transmission system with an optical source being a direct modulated laser since this later presents lighter conception complexity. Nevertheless, the use of such sources for transmission at symbol rates higher than 10 GBaud comes with the drawbacks of having both a poor extinction ratio (which limits the distinction between the states “switch on” and “switch off” at the receiver side) and an additional inherent frequency modulation that impairs the transmission quality.

A telecommunications system consists in three main blocks, a transmitter, a channel and a receiver. In the transmitter block the signal is generated and treated in order to reduce the errors as much as it is possible, in the channel block the signal travels through a particular medium and finally in the receiver block the signal is recovered via different types of techniques. In this case the transmitter is formed by a laser diode and a ring resonator filter; the medium is an optical fiber and the receiver consists on a photodiode, an electrical filter and a clock recovery. The clock recovery gets back the rate of the symbols by giving you a sine signal where each maximum corresponds to the moment where the decision has to be made.

The purpose of a good transmission depends on the errors that exist along the system, if there are fewer errors in one block, there will be fewer errors in the global system. Therefore, if we minimize the error in the transmitter we will have a better transmission, which is the purpose of this project, optimize the transmitter.
In order to do so, the transmitter is formed by a laser diode and a ring resonator filter, and is in this last component where we are going to improve the response of our system.

1.1 OBJECTIVES

The purpose of the project is to optimize the design of an additional integrated optical filter located at the laser output and that takes profit of the frequency modulation of the laser to enhance its extinction ratio. In order to do so, we will perform matlab simulations to find what we may tune in the transfer function of this optical filter to optimize the distance within which an error-free transmission is achieved. We are going to analyze mainly two parameters:

- The value of the slope of the transfer function of the filter at 3dB, which should be between 1dB/GHz and 6dB/GHz.
- The Frequency Spectral Range, FSR, of the filter which should be between 25GHz and 100GHz.

From a knowledge point of view the project will give a more detailed view of the optical direct modulation operation. Besides of analyzing and optimizing those two values, is going to be interesting to reach a BER of around 10^{-9} and also a high extinction ratio (ER) over a low chirp.

This may help in the future design of bidirectional optical link between an end-user computer to the closest optical network node or to facilitate data exchange between server nodes of large-scale datacenters.

2. STATE OF ART

In the last 20 years, the amount of digital information that the client has demanded has grown exponentially, and that is one of the reasons why optical communications have grown in the last decade. One of the advantages of optical communication is to tolerate the transportation of enormous volume of data, typically such as 2.5-10 Gbps rates per channel are used nowadays. This data has been transmitted in the electrical domain so there has to be a component in the system that transforms the voltage into bits. The modulator is the responsible of performing this task by making a conversion from that domain to the optical one before the bits reach the photodiode in the receiver after passing through the fiber. The standard parameters of frequency and transmission window employed in a theoretical modulation are around 194THz and 1550nm:

$$f_0 = \frac{c_0}{\lambda_0} = 194\,THz\ (carrier) \tag{1}$$

At the moment, a simple way to achieve these values in the majority of optical communication systems is by modulating the intensity of the laser.

Nowadays, there are three main technologies used in modulators for optical transmissions. These technologies are in charge of modulating the signal, which consists in transferring the information to be transmitted from the electrical to the optical domain. The first and simplest one allows you to obtain the modulated signal from the direct variation of the polarization current of the laser diode; this process is known as Direct Modulation Laser (DML) and is used in short-range systems. The second technology is based in electro absorption mechanisms, Electro Absorption Modulators (EAM) [5], frequently employed in long-haul systems. The last types of modulators are known as Mach-Zehnder Modulators (MZMs).

The DML consists on changing the polarization current of the laser in order to generate an on/off keying modulation (OOK) at the output of the system. This modulation consists in emitting for each bit of information a certain value of power, a high level when the data is “1” and a low level when is “0”; in this last case the power level could be 0 W although is not desirable. Using this technique we can reach bit rates of 10 Gbps and sometimes 40 Gbps in the laboratory.

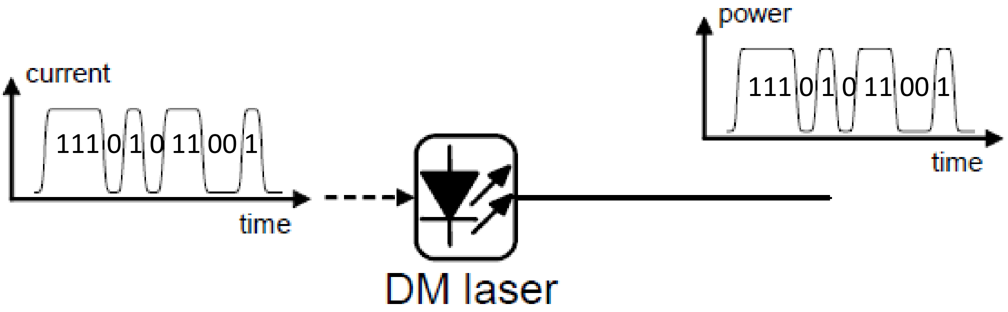

Figure 1: Direct modulation of the laser [5]

By changing the current of polarization of the laser diode the OOK modulation is generated in the semiconductor laser, so the electrical signal is converted into an optical signal.

2.1 NRZ OOK MODULATION

Inside the OOK modulation there exist different ways to codify the signal, such as non-return-to-zero (NRZ) or return-to-zero (RZ). In this case we are going to use the NRZ case because this line code has been the most used system for a long time due to its easy implementation features. Moreover, there are other characteristics that gives some advantages to this format:

- It has a lower bandwidth (BW) compared to the RZ.
- It has immunity against phase noise.
- Its simplicity of implementation allows a simple and cheaper design of the transceiver.

Nowadays, the trend is to create long haul links that can work with high capacities, for example in DWDM systems, which is why the OOK NRZ format has lost power against more efficient systems. However, this line code can work in the 10 Gbps rate without any problem in short-range systems, with DML, and in long-haul systems, with EAM. If we want to make a very long-haul system we should use the MZM, which leads to polarize the modulator with a voltage of half of the output power.

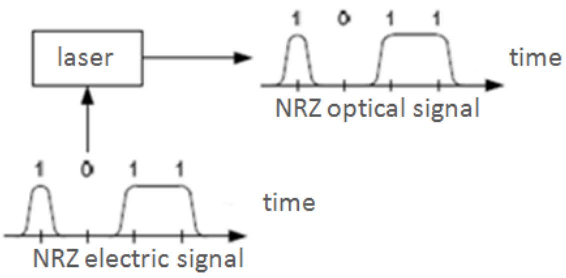

Figure 2: NRZ OOK modulation [2]

In the next figure, the optical spectrum and the eye diagram with no noise and no linearity of a NRZ OOK modulated signal are represented. The optical spectrum is compact but it does not mean that has a better behavior in terms of immunity and chromatic dispersion.

Figure 3: Optical spectrum and eye diagramme of a NRZ OOK signal [2]

2.2 DML BEHAVIOUR

Here it is shown the behavior of a direct modulated laser diode when the goal is to obtain a modulation of the optical output power of the laser.

Different strategies can be employed when it comes to laser modulation, the simplest one is related to the modulation of the amplitude of the optical output power by varying the supply current of the laser. This take place when the laser bias current is between two values, I_1 and I_0, and also over a threshold level. This variation is directly translated into two output power levels P_1 and P_0. The variation of the bias current will be represented as a certain frequency, if this frequency is under a certain value there are not going to be large penalties (although the transmission rate is low); however, if we operate at higher frequency, we should consider other interfering phenomena that will limit the transmission.

To perform a formal study of the direct modulation of a laser diode, we must start from the equation of photon emission rate:

$$\frac{dS}{dt} = \frac{S}{\tau_{ph}}(G - 1) + K_{tot}R_{sp} \tag{2}$$

where the normalized gain G is expressed as:

$$G = R_{st}\tau_{ph} \tag{3}$$

where R_{st} is the stimulated emission rate, τ_{ph} is the photon lifetime, R_{sp} is the rate of spontaneous emission, K_{tot} is the multiplicative total factor of the spontaneous emission and S is the time evolution of the photons emission.
On the other hand, considering the recombination around a carrier threshold density n_{th}:

$$R(n) = R(n_{th}) + \frac{dR}{dn}(n - n_{th}) = R(n_{th}) + \frac{1}{\tau_e}(n - n_{th}) \tag{4}$$

We can give an expression for the charge density around the polarization point as it follows:

$$\frac{dn}{dt} = \frac{I - I_{th}}{eV} - \frac{1}{\tau_e}(n - n_{th}) - \frac{G \cdot S}{V \cdot \tau_{ph}} \tag{5}$$

where I is the instantaneous current, I_{th} is the threshold current, τ_e is the carrier lifetime and V is the volume of the active region of the laser diode. In order to considerate the nonlinear effects in the gain, the following expression arises:

$$G = G_L(1 - k \cdot P) = G_L(1 - k_S \cdot S) \tag{6}$$

where G_L is the linear gain, k is the compression gain factor relative to the optical power, k_S is the compression gain coefficient relative to the number of photons and P is the optical power of the laser.

When a transition from the low current level to the high current level occurs, the optical output power does not vary in an automatic way but in a transitory way. This transitory can have more or less repercussion depending on the value of the low current level. This phenomenon is caused by the application of a current pulse in the laser, then the carrier density increases abruptly over the threshold level and cause a quick increment of photons above the stationary value of the output. This sharply raise of photons over the average level leads to a decrease of the carrier density under the threshold level, which at the same time causes an abrupt diminution of the photons density. This behavior is repeated each time with less variance over the stationary level, so that for a given time ends up converging to itself. This effect will vary depending on where is the low and the high level of current established, giving for each one a certain setup time. This can be easily understood if we consider that when the low setup level of current is under the threshold level, the laser will be switching between the active region to the passive one; so that the population inversion of the carrier will be slower and more abrupt than when the low current level is over the threshold. The expressions of the two cases are shown below:

$$t_s = \tau_e ln\left(\frac{I_{on} - I_{off}}{I_{on} - I_{th}}\right);\ I_{off} < I_{th} < I_{on} \tag{7}$$

$$t_{on} = \frac{\sqrt{2}}{\omega_r}\left[ln\left(\frac{P_{on}}{P_{off}}\right)\right]^{1/2}; I_{th} < I_{off} < I_{on} \tag{8}$$

where ω_r is the resonance frequency of the laser. This frequency can be expressed as follows [6]:

$$\omega_r = \sqrt{\left(\frac{dG}{dn}\right) \cdot \frac{I_{on} - I_{th}}{eV} \cdot \frac{1}{\tau_{ph}}} = \frac{1}{\tau_{ph}}\sqrt{\left(\frac{dG}{dn}\right) \cdot \frac{S_{on}}{V}} \tag{9}$$

In order to obtain the output power of the laser, we are going to explain here the steady state operation. There are two rate equations, one for the carrier number (N), and the other one for the photon number (P) [7]:

$$\frac{dP}{dt} = GP + R_{sp} - \frac{P}{\tau_p} \tag{10}$$

$$\frac{dN}{dt} = \frac{I}{e} - \frac{N}{\tau_c} - GP \tag{11}$$

where G is the net rate of stimulated emission, R_{sp} is the rate of spontaneous emission, I is the intensity of the current, e is the charge of an electron and τ_p and τ_c are respectively the photon lifetime and the carrier lifetime.
There is also an approximation of the peak material gain [7]:

$$g_m = \frac{\tau_g}{V}(N - N_0) \tag{12}$$

where V is the volume of the active region of the laser, τ_g is the differential gain and N_0 is the carrier number at transparency. The net rate of stimulated emission can be approximated to [7]:

$$G = G_N(N - N_0) \tag{13}$$

In the steady state operation the current applied to the laser is constant and also the rate of spontaneous emission is zero [7]:

$$\frac{dN}{dt} = 0, \quad \frac{dP}{dt} = 0, \qquad P = \left(G - \frac{1}{\tau_p}\right) \tag{14}$$

One of the solutions of this equation is $G = \frac{1}{\tau_p}$ so the number of photons is:

$$P = \frac{\tau_p}{e}(I - I_{th}) \tag{15}$$

The power emitted by the laser is:

$$P_e = \frac{1}{2} v_g \alpha_{mir} h\omega P \tag{16}$$

With the expression 15 in the 16 we obtain the power:

$$P_e = \frac{1}{2} \eta_g (I - I_{th}) \frac{hf}{e} \tag{17}$$

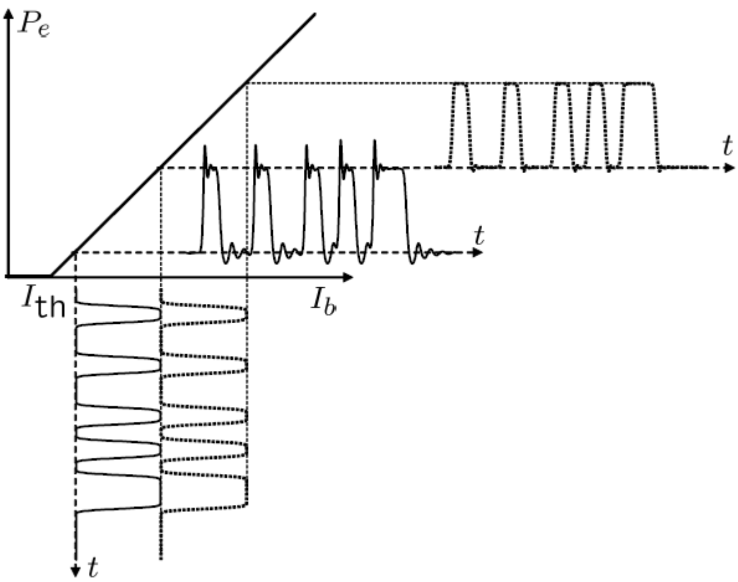

Figure 4: Direct modulation of a semiconductor laser

The laser does not send any information until it reaches the threshold current. When it does, it starts to send the current signal as an optical power. In the figure 4 is also shown a variation of the current which is converted in a variation of the output power of the laser.

2.3 MODULATION TECHNIQUE REQUIREMENTS

There are several requirements in the modulation technique that should be evaluated, such as the speed of operation, the extinction ratio and the frequency chirping. As we have discussed above, in order to have the desired bit rate we need physical processes fast enough to vary from the logical “0” to the logical “1”. So the speed of operation can be seen in time, how long does it take to make one transition? For our bit rate of 10 Gbps the transmitter has to switch between states in duration of 100 ps.

The extinction ratio is defined as the relation of two different power levels [5]:

$$ER = \frac{P_1}{P_0} \tag{18}$$

where P_1 corresponds to the power level of sending a high level “1” and P_0 corresponds to low level “0”. The relation describes itself the separation between the two power levels, and as usually in telecommunications, it is very important to reach a good value. How good is a value of an extinction ratio? The bigger it is, the better it gets. In DML the normal rates for the extinction ratio are going to be varying between 3 dB and 5 dB.

However the consequence of a bad extinction ratio is the appearance of power penalty at the receiver. Since the extinction ratio is a comparison of two power levels, if we only take into account thermal limitations in the receiver, the power penalty can be expressed as:

$$\delta_{ER(dB)} = 10log_{10}\left(\frac{ER+1}{ER-1}\right) \tag{19}$$

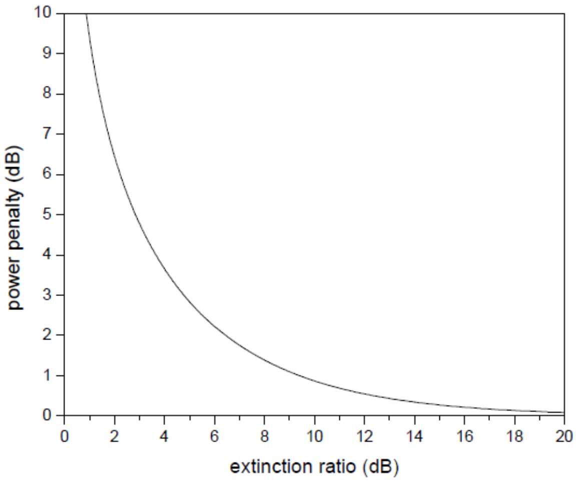

Figure 5: Power penalty VS Extinction Ratio [5]

The last requirement is the frequency chirping, known as chirp, when we want to reach high speed values. This phenomenon is the responsible of the spectral broadening of the signal at the output of the laser and it is quite harmful for DWDM systems, because the adjacent channels will overlap. In order to understand the concept of frequency chirping, we need to revise some concepts.

In the end, everything can be reduced at the level of electric signals and the electric field of a wave is:

$$E(t) = \Re[A(t)e^{i\omega_0 t}] \tag{20}$$

where the expression represents the real part of the complex envelope, A (t). This envelope is a complex number so it can be decomposed in module and phase:

$$A(t) = |A(t)|e^{i\phi(t)} = \sqrt{P(t)}e^{i\phi(t)} \tag{21}$$

where the module of the envelope is the power of the signal. As it has been explained before, DML is sort of an intensity modulation because by modifying it you can vary the power of the laser, P (t) in this case. Nevertheless, as a lot of things in life, nothing is perfect; this means that one variation in the intensity translates into a variation in the power and also in the phase ϕ. Therefore the phase, like the power, begins to depend on time; so the frequency adds a variable component to its expression:

$$\omega(t) = \omega_0 + \frac{\partial\phi}{\partial t} \tag{22}$$

and is this component what makes the laser modulate the frequency, not just the power. This phenomenon is called frequency chirping.

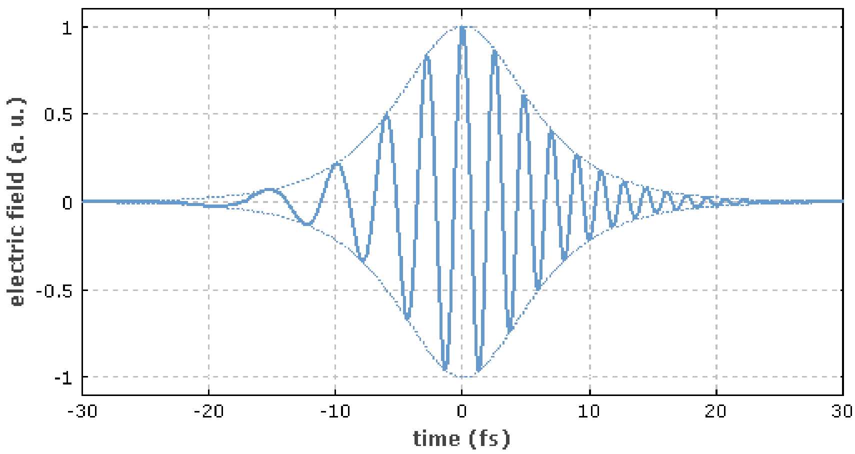

Figure 6: Frequency chirping

The transmission rate in this project is 10 Gbps and the frequency carrier is 194 THz, almost 200 THz, which means is nearly 20000 times bigger than the bandwidth so the effect of the chirp is important to take into account. The chirp is inherent in a direct modulated laser environment and since it consists in a variation of the frequency it can be represented as:

$$\Delta f(t) = \frac{\alpha}{4\pi}\left(\frac{d}{dt}[lnP_e(t)] + kP_e(t)\right) \quad (23)$$

where α is the linewidth enhancement factor and k is the adiabatic chirp. The chirp has two components, the adiabatic chirp and the transient chirp, the first one is proportional to the power and the second one varies with the variation of the power in time.

3. OPTIMISATION OF THE FILTER

3.1 INTRODUCTION

In this project the goal is to optimize the characteristics of an optical ring resonator filter situated after the transmitter, the laser. This complex structure that is directly in relation to the Fabry-Pérot theory [8], is going to improve the response of the system and decrease the BER in the receiver. Nowadays the ring resonators are used in cascade in a lot of implementations but in this project we are going to analyze the behavior of a single ring resonator.

3.2 RING RESONATOR

In this section our goal is to obtain the transfer function of the filter. Once we get to this equation we are able to optimize the filter with the factors involved in it, and in order to do so we need to start from the theoretical background of a ring resonator. A single ring resonator has a configuration which consists on a waveguide and a circle (ring) with a radius r as follows:

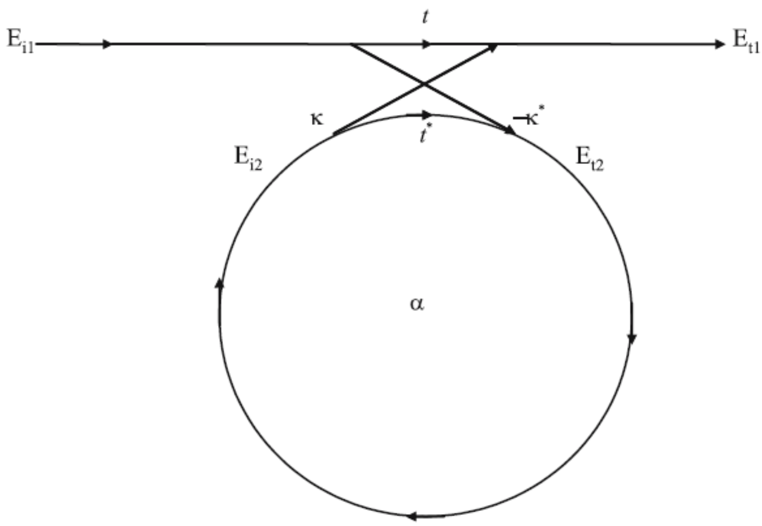

Figure 7: Single Ring Resonator [9]

This figure shows the geometry of a single ring resonator with lossless coupling between the waveguide and the ring, the interaction follows the next matrix equation [9]:

$$\begin{pmatrix} E_{t1} \\ E_{t2} \end{pmatrix} = \begin{pmatrix} t & k \\ -k^* & t^* \end{pmatrix} \cdot \begin{pmatrix} E_{i1} \\ E_{i2} \end{pmatrix} \tag{24}$$

where as it is shown in the figure 5 there are two different complex mode amplitudes, E_{tj} and E_{ij}, which are the transmitted mode amplitude and the incident mode amplitude respectively (where j is the number of the port). There are two coupler parameters, t and k (and their respectively conjugated complex values k^* and t^*), depending on the mechanism employed. Since the networks are reciprocal, the matrix is symmetric and we can assume [9]:

$$|k^2| + |t^2| = 1 \tag{25}$$

The equation 24 is still complicated; therefore if the input wave E_{i1} is equal to 1 the field amplitudes will be normalized and the model will be simplified [9]:

$$E_{i2} = \alpha \cdot e^{j\theta} \cdot E_{t2} \tag{26}$$

This equation 26 shows the transmission around the ring resonator where α represents the internal losses in the ring, being $\alpha = 1$ no losses, and:

$$\theta = \frac{\omega L}{c} \tag{27}$$

where:

$$\omega = k \cdot c_0 \tag{28}$$

$$k = \frac{2\pi}{\lambda} \tag{29}$$

$$L = 2\pi r \tag{30}$$

$$c = \frac{c_0}{n_{eff}} \tag{31}$$

where ω is the angular frequency, the radius r of the circumference of the ring (measured from the center of the waveguide to the center of the ring) is represented by the L parameter, c is the phase velocity and by definition c_0 is the vacuum speed of light and n_{eff} is the effective refractive index. The equation 29 shows the vacuum wave number, and if we multiply it by the effective refractive index we will obtain the propagation constant [9]:

$$\beta = k \cdot n_{eff} \tag{32}$$

With these equations we can simplify the equation 27 and obtain:

$$\theta = \frac{\omega L}{c} = \frac{k \cdot c_0 \cdot L}{c} = \frac{2\pi \cdot c_0 \cdot L}{c \cdot \lambda} = \frac{2\pi \cdot n_{eff} \cdot L}{\lambda} = \frac{2\pi \cdot n_{eff} \cdot L \cdot f}{c_0} \tag{33}$$

where we have substituted:

$$\lambda = \frac{c_0}{f} \tag{34}$$

in order to make the transfer function of the filter depends on the frequency to represent our results along the frequency axis. Now, from the equations 24 and 26 we can obtain the transfer function of the ring resonator [4]:

$$E_{t1} = \frac{-\alpha + t \cdot e^{-j\theta}}{-\alpha t^{*} + e^{-j\theta}} \tag{35}$$

and also the transmission around the ring [4]:

$$E_{i2} = \frac{-\alpha k^{*}}{-\alpha t^{*} + e^{-j\theta}} \tag{36}$$

The transfer function of our filter is going to be described by the equation 35 where $t = |t|e^{j\varphi_t}$. The phase of the coupler is represented by $\varphi_t$and the coupling losses by $|t|$. Since we have obtained the mode amplitude we can also find the transmitted power [9]:

$$P_{t1} = |E_{t1}|^2 = \frac{\alpha^2 + |t|^2 - 2\alpha|t|\cos\left(\theta + \varphi_t\right)}{1 + \alpha^2|t|^2 - 2\alpha|t|\cos\left(\theta + \varphi_t\right)} \tag{37}$$

It is significant to mention that the majority of the remarkable characteristics of this single ring resonator take place near the resonance where [4]:

$$(\theta + \varphi_t) = m2\pi \tag{38}$$

where m is an integer. If we now simplify the transmitted power (equation 37) as follows [9]:

$$P_{t1} = |E_{t1}|^2 = \frac{(\alpha - |t|)^2}{(1 - \alpha|t|)^2} \tag{39}$$

There is a special case to consider in the equation 39, if we are near resonance and $\alpha = |t|$ then the transmitted power will be 0. This phenomenon is known as critical coupling and is produced when the two losses factors are equal because of the destructive interference.

From now on some parameters are going to be presented in order to understand the behavior of the ring resonator and then the experimental work will be displayed.

3.3 PARAMETERS

There are mainly three parameters that help us to describe the behavior of the ring resonator, and they are the free spectral range, the full width at half maximum and the finesse.

3.3.1 Free Spectral Range (FSR)

The free spectral range, FSR, is the distance in frequency or wavelengths between two maximums. In our case of study the maximums will be placed were the resonance takes place, we can observe it in the following figure:

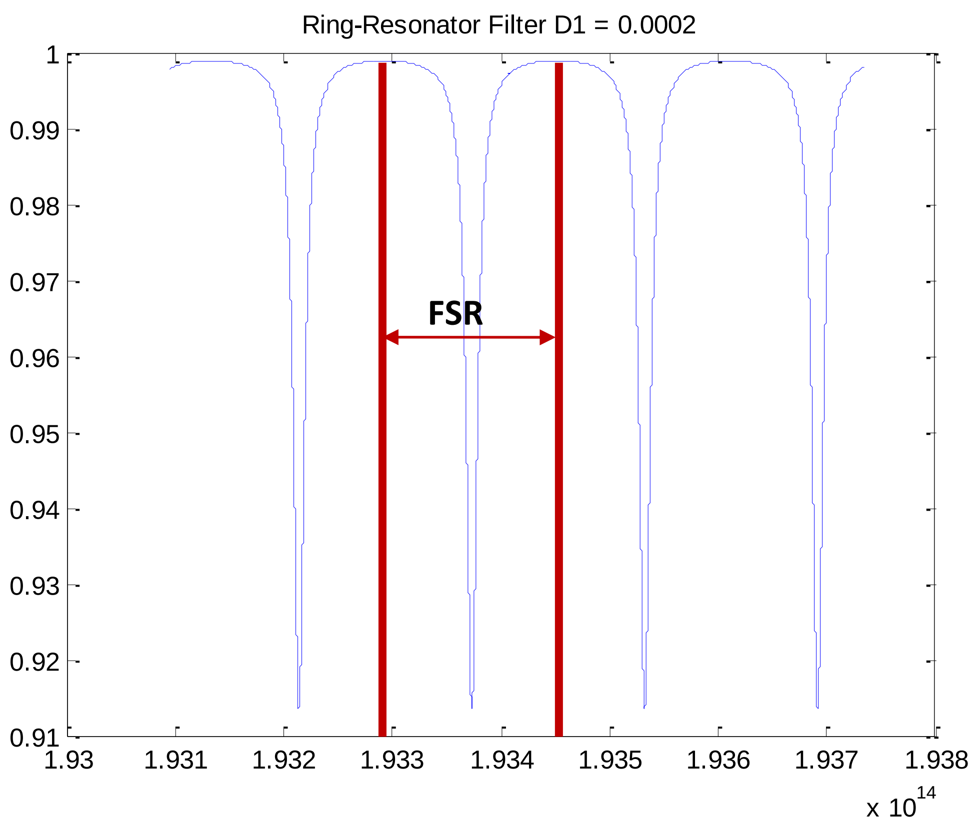

Figure 8: Free Spectral Range

The mathematical form of the FSR in the frequency domain is:

$$\Delta \upsilon = \frac{c}{n_{eff} L} \tag{40}$$

and in the wavelength domain [9]:

$$\Delta \lambda = \frac{\lambda^2}{n_{eff} L} \tag{41}$$

It is highly remarkable that the FSR varies inversely with the length of the ring circumference. We can simplify this concept saying that for smaller radius of the ring the FSR will get wider and wider.

3.3.2 Full width at half maximum (FWHM)

The full width at half maximum (FWHM) is the 3dB bandwidth and it can be expressed as [9]:

$$FWHM = 2\delta\lambda = \frac{\kappa^2\lambda^2}{\pi L n_{eff}} \tag{42}$$

3.3.3 Finesse (F)

Finally the finesse (F) is the ratio between the FSR and the FWHM and it's a measure of the frequency selectivity:

$$F = \frac{FSR}{FWHM} \approx \frac{\pi}{\kappa^2} \tag{43}$$

If there is a high value of the finesse it means that we have narrow peaks, so for very selective filters is preferable to obtain high values of the finesse.

3.4 EXPERIMENTAL WORK AND RESULTS

Before starting any simulation we have to describe the parameters of the environment where the filter is going to be placed. The frequency, the wavelength and the transfer function has been previously explained but let remember the values:

$$f_0 = \frac{c_0}{\lambda_0} = 194\ THz\ (carrier) \tag{1}$$

with $\lambda_0 = 1550nm$ and:

$$T(f) = E_{t1} = \frac{-\alpha + t \cdot e^{-j\theta}}{-\alpha t^* + e^{-j\theta}} \tag{35}$$

We can observe that in the transfer function there are three degrees of freedom, the internal loss α, the coupling loss t and the length of the ring circumference L. The fixed parameters are the frequency and the refractive index n_{eff}. The frequency range in order to integrate the filter in the global system has to be the same, around the 194 THz value, to be exact:

$$193.0944890322581\ THz < f < 193.7344865908518 \tag{44}$$

where the values of the maximum frequency and the minimum frequency are respectively $193.7344865908518\ THz$ and $193.0944890322581\ THz$.

For this analysis we are going to delimit the FSR values near 25 GHz, 50 GHz and 100 GHz, and the values of the slope of the transfer function of the filter related to the finesse are from 1dB/GHz to 6dB/GHz. The procedure to estimate the value of the slope of the filter is to calculate the derivative of the transfer function and make it equal to zero:

$$slope = \frac{dT(f)}{df} = 0 \tag{45}$$

There are three degrees of freedom which means that we have to fix one of them, and in this case the coupling loss is fixed to 0.99 [4].

The refractive index depends on the material where the ring resonator filter is built in. There are two main elements where it is manufactured, the Crystalline Silicon (Si) and the Silicon dioxide (SiO2). The variation of the index depends on the wavelength as it follows:

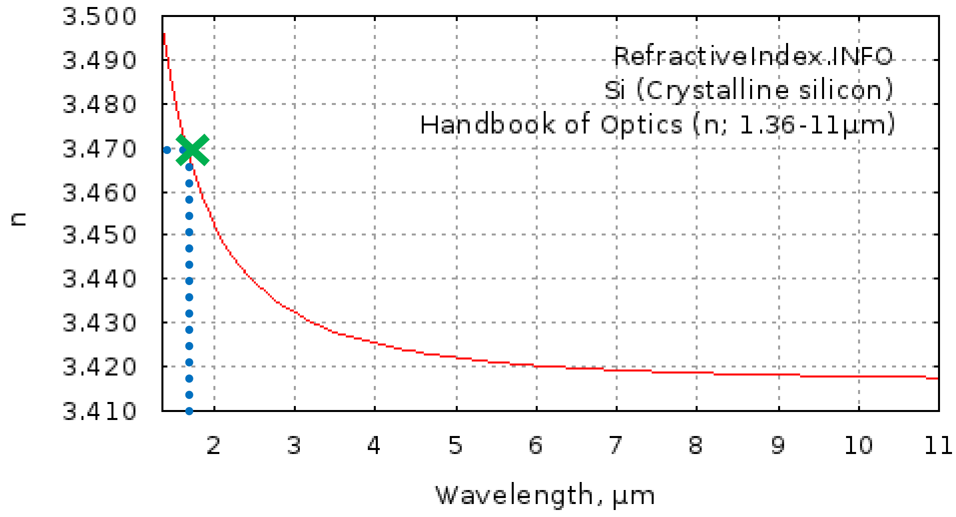

Figure 9: Refractive index in Si

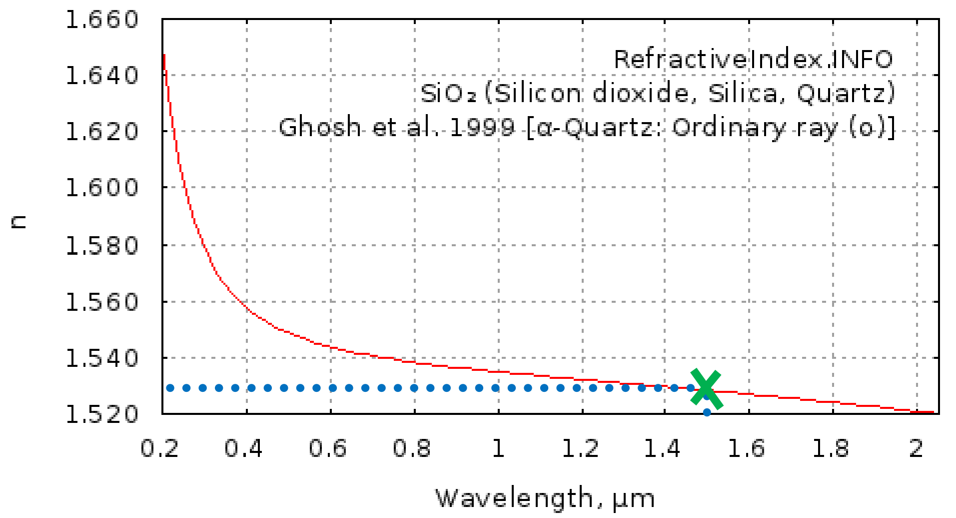

Figure 10: Refractive index in SiO2

For our wavelength value (1550 nm), there are two refractive indexes, one for each material marked with a green cross by the blue lines:

$$n_{Si} = 3.4777 \tag{46}$$

$$n_{SiO2} = 1.5277 \quad (47)$$

In this project we have set the coupling factor to 0.99 so the only degrees of freedom are the internal loss and the length of the ring. In order to analyze the behavior of the filter we are going to vary one parameter while we maintain the other one fixed. In the following graphs we fix the diameter of the ring to $200\,\mu m$ and change the internal loss coefficient:

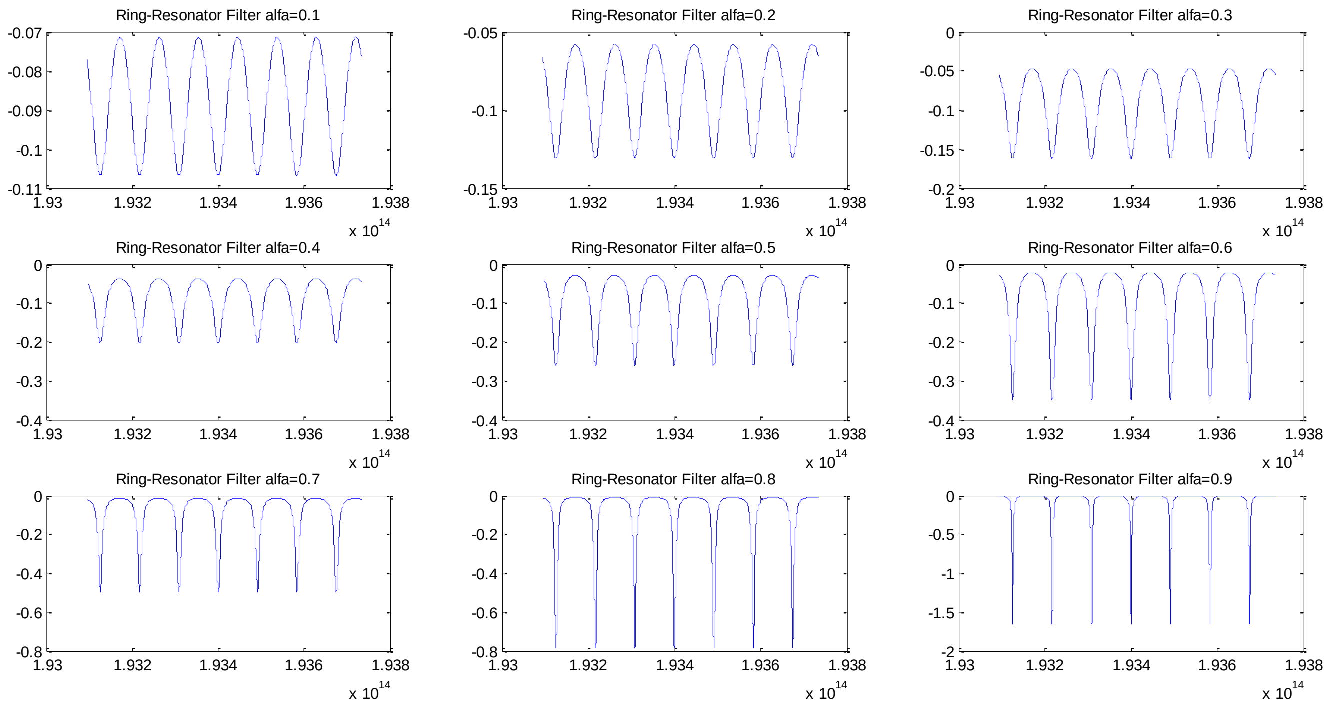

Figure 11: Filter response by varying the internal loss from 0.1 to 0.9 with n=3.4777

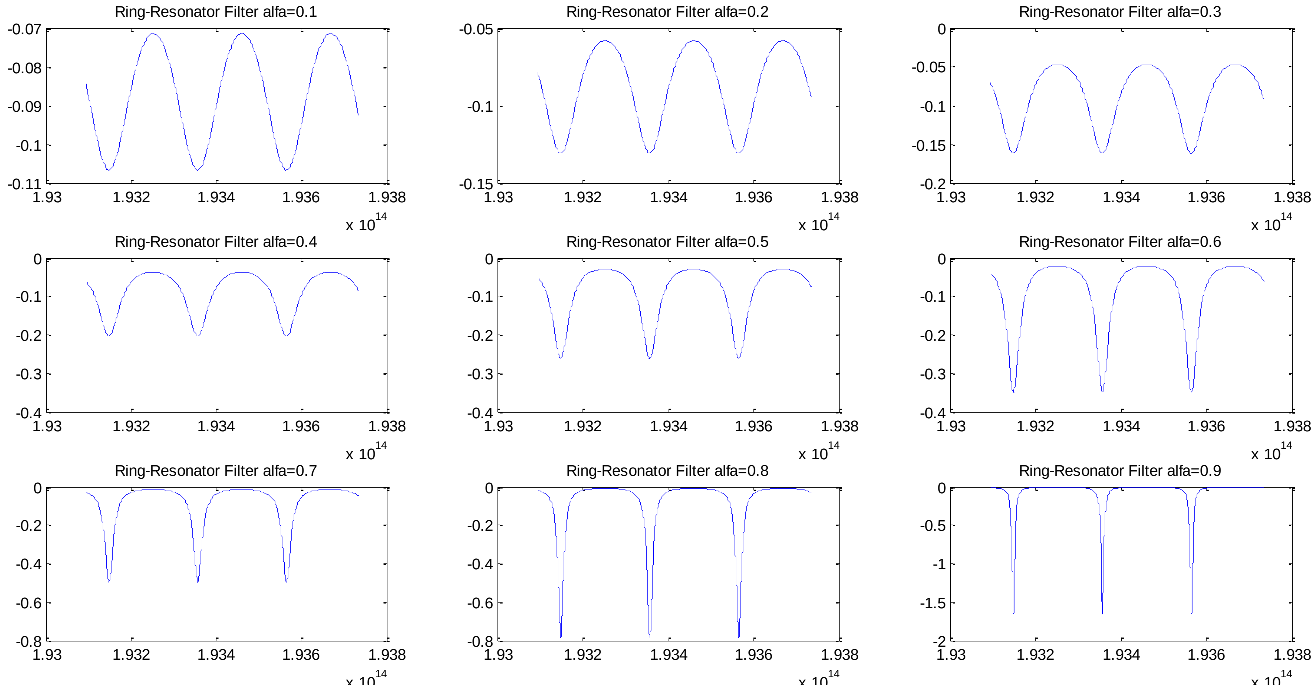

Figure 12: Filter response by varying the internal loss from 0.1 to 0.9 with n=1.5277

As we have mentioned before in the theoretical part, the FSR gets wider when the length of the circumference increases (expression 40), and also when the refractive index does it. Therefore we choose the equation 46, $n_{Si} = 3.4777$, because our FSR is limited from 25 to 100 GHz and we have experimented that for lower values of the diameter of the ring the FSR is in the interval with the crystalline silicon refractive index.

The purpose of the figures 9 and 10 is to show the change of the transfer function when the internal loss coefficient is varying from 0.1 to 0.9. in both cases, crystalline silicon and silicon dioxide, the filter starts to have a better response when alpha is 0.8. From 0.9 to 0.98 the response is even more accurate:

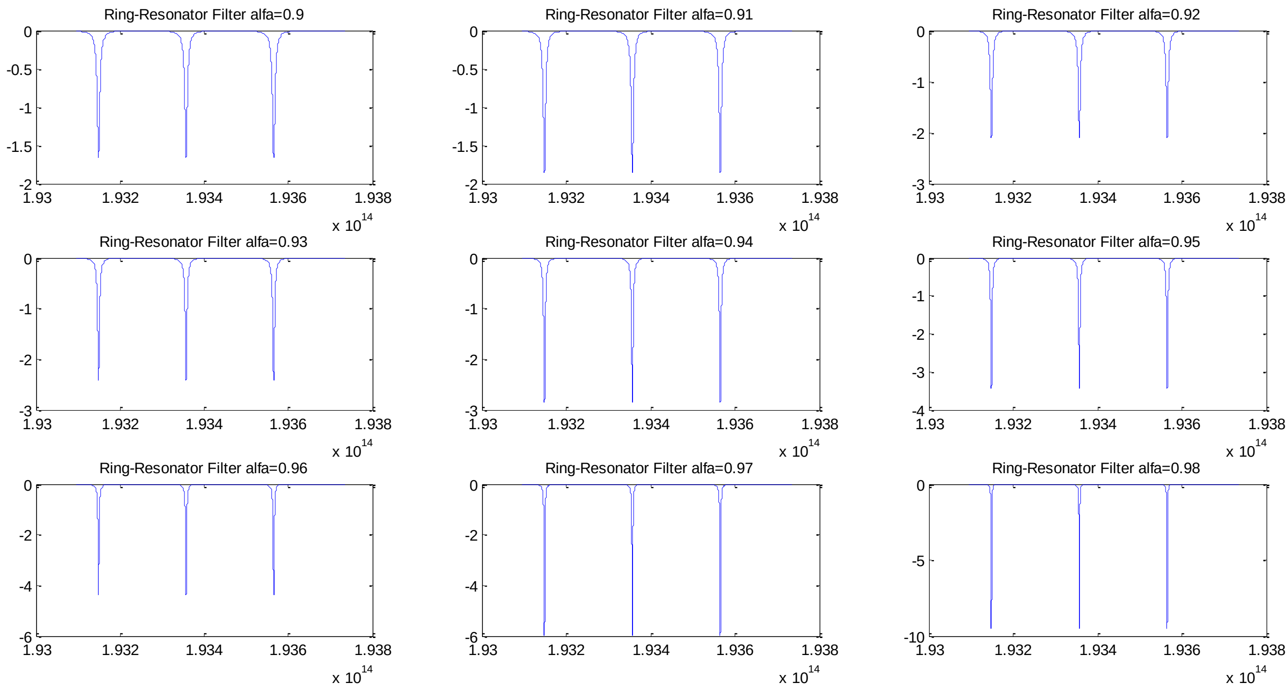

Figure 13: Filter response by varying the internal loss from 0.9 to 0.98 with n=3.4777

Taking a look to the figure 11 we cannot determine which value is better for the filter, we will have to introduce more elements to the equation. We have modified the internal loss coefficient and found that we can work in the interval of 0.8 to 0.9. So now we fix the internal loss coefficient to 0.95, which is a medium value between 0.9 and 0.99 and we change the diameter of the ring starting by 50 μm [10]:

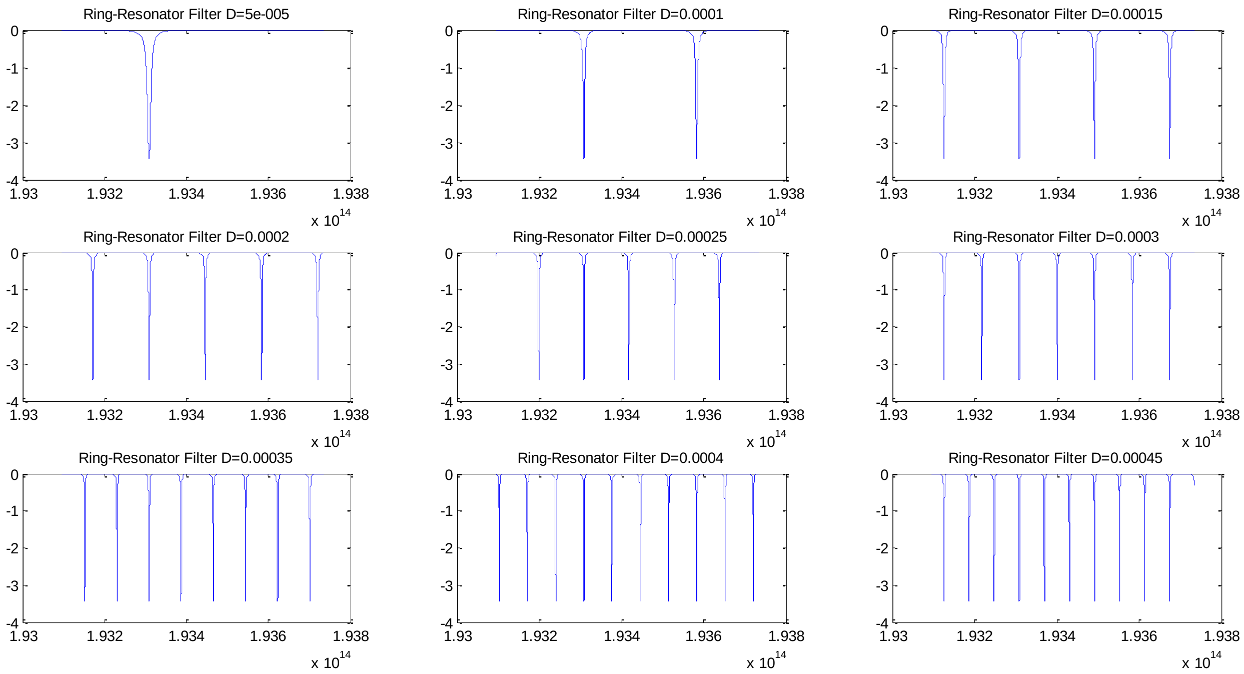

Figure 14: Filter response by varying the diameter of the ring from 50um to 450um with n=3.4777

As it was expected the FSR gets narrower when the diameter of the ring grows. The goal now is to observe the evolution of these two parameters, the internal losses and the diameter of the ring, when we try to obtain the correspondent values for FSR and finesse.

We have discussed in the theoretical part the dependence of the FSR and the transfer function. Since the slope of the filter, m, depends directly on the transfer function of the filter, it is going to vary in function of t, α, L and n_{eff}. On the other hand the FSR varies with L and n_{eff}. In this experimental part we have fixed two of the four parameters, the coupling factor and the refractive index. With this new scenario the dependence changes, FSR (L) and m (α, L).

In the figures 15 and 16 it is shown the response of the filter for a given case of internal loss of 0.93 and diameter of 550 μm. These two values make the filter reach a FSR of 49.9 GHz and a slope value of 2.7 dB/GHz. It is also very well appreciated how the maximums of the derivative are situated in the zeros of the transfer function.

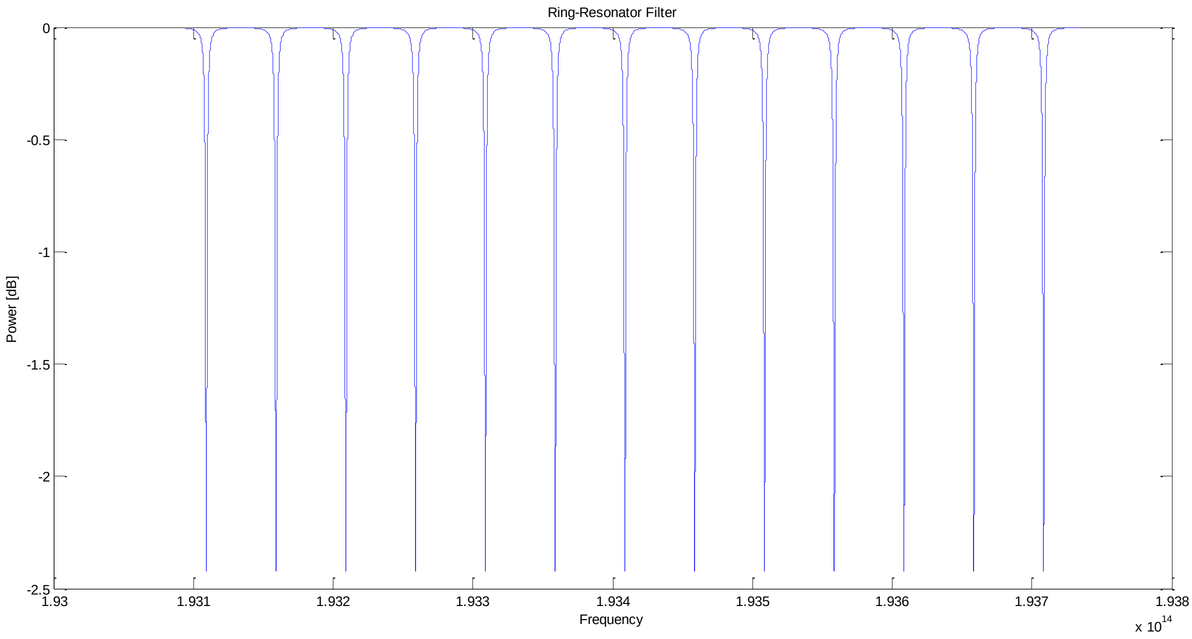

Figure 15: Ring resonator filter response with an internal loss of 0.93 and a diameter of 550um

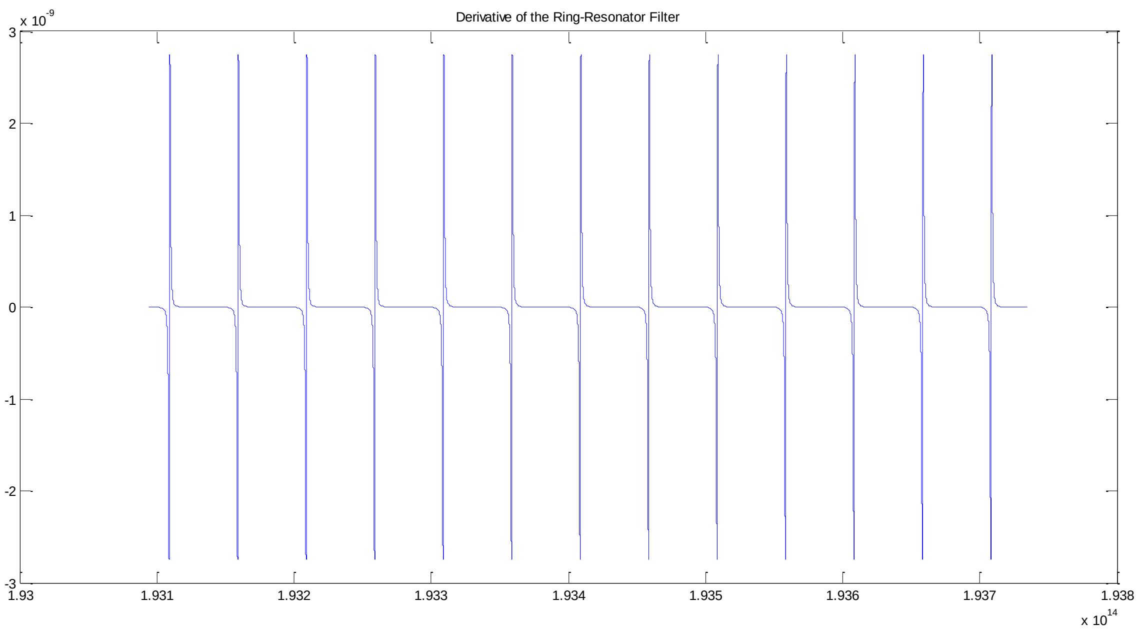

Figure 16:Derivative of the ring resonator with internal loss of 0.93 and diameter of 550um

In order to analyze the most accurate values of the diameter and the internal losses we are going to display some charts with all the simulations and the values of each parameter when the coupling factor and the refractive index are fixed to 0.99 and 3.4777 respectively.

3.4.1 SIMULATION RESULTS

$Diameter\ (\mu m)$	α	$Slope\ (\frac{dB}{GHz})$	$FSR\ (GHz)$
250	0.90	0.6	109.8
250	0.91	0.7	109.8
250	0.92	0.9	109.8
250	0.93	1.2	109.8
250	0.94	1.7	109.8
250	0.95	2.5	109.8
250	0.96	4.1	109.8

$Diameter\ (\mu m)$	α	$Slope\ (\frac{dB}{GHz})$	$FSR\ (GHz)$
300	0.90	0.7	91.5
300	0.91	0.9	91.5
300	0.92	1.1	91.5
300	0.93	1.5	91.5
300	0.94	2.1	91.5
300	0.95	3	91.5
300	0.96	4.9	91.5

$Diameter\ (\mu m)$	α	$Slope\ (\frac{dB}{GHz})$	$FSR\ (GHz)$
350	0.90	0.8	78.5
350	0.91	1	78.5
350	0.92	1.3	78.5
350	0.93	1.7	78.5
350	0.94	2.4	78.5
350	0.95	3.6	78.5
350	0.96	5.7	78.5

$Diameter\ (\mu m)$	α	$Slope\ (\frac{dB}{GHz})$	$FSR\ (GHz)$
400	0.90	0.9	68.6
400	0.91	1.2	68.6
400	0.92	1.5	68.6
400	0.93	2	68.6
400	0.94	2.8	68.6
400	0.95	4.1	68.6
400	0.96	6.5	68.6

$Diameter\ (\mu m)$	α	$Slope\ (\frac{dB}{GHz})$	$FSR\ (GHz)$
450	0.90	1.1	61
450	0.91	1.3	61
450	0.92	1.7	61
450	0.93	2.2	61
450	0.94	3.1	61
450	0.95	4.6	61
450	0.96	7.3	61

$Diameter\ (\mu m)$	α	$Slope\ (\frac{dB}{GHz})$	$FSR\ (GHz)$
500	0.90	1.2	54.9
500	0.91	1.5	54.9
500	0.92	1.9	54.9
500	0.93	2.5	54.9
500	0.94	3.5	54.9
500	0.95	5.1	54.9
500	0.96	8.2	54.9

$Diameter\ (\mu m)$	α	$Slope\ (\frac{dB}{GHz})$	$FSR\ (GHz)$
550	0.90	1.3	49.9
550	0.91	1.6	49.9
550	0.92	2.1	49.9
550	0.93	2.7	49.9
550	0.94	3.8	49.9
550	0.95	5.6	49.9

$Diameter\ (\mu m)$	α	$Slope\ (\frac{dB}{GHz})$	$FSR\ (GHz)$
600	0.90	1.4	45.8
600	0.91	1.8	45.8
600	0.92	2.3	45.8
600	0.93	3	45.8
600	0.94	4.1	45.8
600	0.95	6.1	45.8

$Diameter\ (\mu m)$	α	$Slope\ (\frac{dB}{GHz})$	$FSR\ (GHz)$
650	0.90	1.5	42.2
650	0.91	1.9	42.2
650	0.92	2.5	42.2
650	0.93	3.2	42.2
650	0.94	4.5	42.2
650	0.95	6.6	42.2

$Diameter\ (\mu m)$	α	$Slope\ (\frac{dB}{GHz})$	$FSR\ (GHz)$
700	0.90	1.6	39.2
700	0.91	2.1	39.2
700	0.92	2.6	39.2
700	0.93	3.5	39.2
700	0.94	4.8	39.2

$Diameter\ (\mu m)$	α	$Slope\ (\frac{dB}{GHz})$	$FSR\ (GHz)$
750	0.90	1.8	36.6
750	0.91	2.2	36.6
750	0.92	2.8	36.6
750	0.93	3.7	36.6
750	0.94	5.2	36.6

$Diameter\ (\mu m)$	α	$Slope\ (\frac{dB}{GHz})$	$FSR\ (GHz)$
800	0.90	1.9	34.3
800	0.91	2.4	34.3
800	0.92	3	34.3
800	0.93	4	34.3
800	0.94	5.5	34.3

$Diameter\ (\mu m)$	α	$Slope\ (\frac{dB}{GHz})$	$FSR\ (GHz)$
850	0.90	2	32.3
850	0.91	2.5	32.3
850	0.92	3.2	32.3
850	0.93	4.2	32.3
850	0.94	5.9	32.3

After this results is remarkable to say that when the diameter increases, the slope of the transfer function of the filter increases too which means they are directly proportional. In fact, as the diameter reaches higher values, in order to remain in the same slope interval and have the same features, we will have to peak lower values of the internal loss α. The lower value of the diameter that we can work with is around $250\ \mu m$ because otherwise the FSR would be over its maximum. The higher value of the diameter is not shown in these charts because it is very high, $1100\ \mu m$, the same thing happens with the lowest value of the internal loss (0.85).

Therefore the diameter and the internal loss vary given the following intervals:

$$250\ \mu m \leq Diameter \leq 1100\ \mu m \tag{48}$$

$$0.85 \leq \alpha \leq 0.96 \tag{49}$$

It is interesting to see also the exponential behavior of the FSR against the diameter of the ring to verify the theoretical equation:

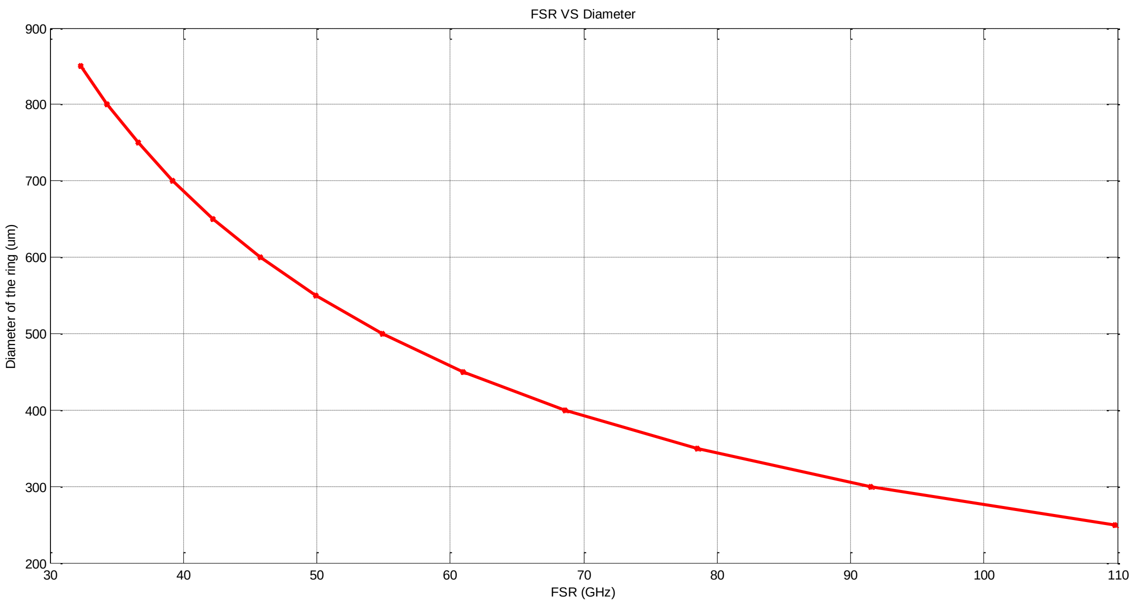

Figure 17: FSR VS Diameter of the ring

4. CONCLUSION

In this project it has been studied the behavior of a ring resonator filter in a short-range optical environment where the transmitter is a direct modulated semiconductor laser. At first, in order to carry out all the analysis, some theoretical backgrounds of DML and NRZ OOK modulation have been explained. Even though DML is a simple way of modulation from the electrical plane to the optical plane, for this particular case, is adequate; because the system where the filter is going to be placed in has a bit rate of 10 Gbps, which is reachable for this particular technology.

A deeply analysis has been carried out by studying the behavior of different parameters of the ring resonator such as the length of its circumference, the internal losses, the coupling factor, the refractive index, the FSR or the slope of the transfer function of the filter (which is related to the finesse). We had to perform a meticulous investigation in order to keep the intervals of both FSR and slope of the transfer function of the filter. It has been demonstrated that by varying just the internal loss and the length of the ring resonator, the initial conditions are still satisfied.

At the end, we carried out a very complete analysis for the optimization of a ring resonator filter in a short-range optical link environment concluding that it is possible to achieve a good value for the diameter of the ring and the internal losses while the distance of an error-free transmission is optimized.

ANNEXES: Transfer function matlab code

```
n=3.4777;
c0 = 3e8;

freq_min = 1.930944890322581e14;     %193.094 THz
freq_max = 1.937344865908518e14;     %193.734 THz

lengthFreq = 262144;

D1=250e-6;            %Diameter of the ring (250um)

L=pi*D1;              %Perimeter of the ring

t=0.99;                %coupling losses
beta = 0.96;           %internal losses

Nb = lengthFreq;

paso = (freq_max-freq_min)/Nb;


for beta=0.9:0.01:0.97

    i=1;
    j=1;

    freq = freq_min:(freq_max-freq_min)/Nb:freq_max-(1/Nb);
    theta = 2*pi*n*L*freq./c0;

    %Funcion de transferencia del filtro
    R = (-beta+t*exp(-1i*theta))./(-beta*t+exp(-1i*theta));

    %Calculo la derivada
    Rmodulo = abs(R).^2;

    Rderiv = diff(10*log10(Rmodulo))./paso;
    Rderiv = [Rderiv 0];

    %Calculo el valor en dBs de la pendiente de la derivada
    MaximoDerivada = max(abs(Rderiv));

    %Calculo el FSR
    [valor1,location1] = findpeaks(abs(R).^2);
    location = zeros(1,length(location1)-1);

    for i=2:1:length(location1)
        location(j) = location1(i)-location1(j);
        j = j+1;
    end
    Location = min(location);
    FSR = paso*Location;

end
```

BIBLIOGRAPHY

[1] Govind P. Agrawal, “Fiber-Optic Communications Systems”, Third Edition, Wiley-Interscience. <http://nora.ing.unibs.it/riservato/com_ottiche/materiale/>

[2] Adolfo Lerín y de la Santísima Trinidad, “Modulación directa de diodos láser de alta velocidad para sistemas de transmisión coherente”, Proyecto Final de Carrera.

[3] Marcel Elshoff, Oscar Rautenberg, “Design and modelling of ring resonators used as optical filters for communications applications”, Bachelorarbeit.

[4] A. Yariv, “Universal relations for coupling of optical power between microresonators and dielectric waveguides", ELECTRONICS LETTERS 17th February 2000 Vol. 36 No. 4.

[5] Christophe Peucheret, “Direct and External Modulation of Light”, DTU Fotonik, Department of Photonics Engineering, Technical University of Denmark.

[6] John M. Senior, “Optical Fiber Communications Principles and Practice”, Third Edition, Pearson Prentice Hall.

[7] Christophe Peucheret, “Direct Current Modulation of Semiconductor Lasers”, DTU Fotonik, Department of Photonics Engineering, Technical University of Denmark.

[8] H. van de Stadt, J. M. Muller, “Multimirror Fabry-Perot Interferometers”, Journal of the Optical Society of America -A, Vol.02, (08), 1363-1370, (1985)

[9] Dominik G. Rabus, “Integrated Ring Resonators”, Springer, 2007.

[10] Xudong Fan, Ian M. White, Hongying Zhu, Jonathan D. Suter, and Hesam Oveys, “Overview of novel integrated optical ring resonator bio/chemical sensors”, Biological Engineering Department, University of Missouri 1201 E. Rollins Street, 240D Life Sciences Center, Columbia, MO 65211.